





Laboratory Report of

National Metrology Institute of Japan (NMIJ/AIST)

and Japan Electric Meters Inspection Corporation (JEMIC)

2023-2025

At NMIJ/AIST, there are five research groups in the electrical standards area. They are the Applied Electrical Standards Group, the Quantum Electrical Standards Group, the Radio-Frequency Standards Group, the Electromagnetic Fields Standards Group, and the Electromagnetic Measurement Group.

The Applied Electrical Standards Group takes charge of the AC/DC transfer, the impedance and the power standards. The Quantum Electrical Standards Group covers the Josephson voltage and the quantum Hall resistance standards.

The Radio-Frequency Standards Group takes charge of RF power, voltage, noise, and attenuation standards. The Electromagnetic Fields Standards Group covers antenna properties, electric field and magnetic field standards. The Electromagnetic Measurement Group takes charge of RF impedance (S-parameter) standards and material properties.

JEMIC maintains the national standards of electrical power as DI and provides calibration services for electrical, thermal, photometric, etc. instruments using various secondary standards under the Japan Calibration Service System scheme.

This report also includes an overview of the digitalization projects undertaken at NMIJ and their specific implementation in the area of electrical standards as in the last section.

1. Josephson Voltage

1.1 PJVS operation in dilution refrigerator system

A liquid-helium-free PJVS cooled with a GM cooler has been utilized since 2015 for calibrations of Zener voltage standards with the CMC values, 8 nV for 1 V and 45 nV for 10 V, same as those for our conventional JVS system cooled with liquid helium. We are now attempting to operate the PJVS chip on the 4 K stage in a dilution refrigerator system toward the quantum-metrology-triangle measurement and other general applications. We have succeeded in the stable temperature control of the sample stages and the stable generation of the quantized voltage steps with the relative standard uncertainty of 2.4×10^{-10} for nominal 1 V output [1a]. Then, we developed a superconducting magnetic shield





structure and installed it to the 4 K stage in the dilution refrigerator. As a result, we confirmed stable Shapiro steps in the *I-V* characteristics of a PJVS device covered with the shielding structure in a magnetic-field environment [1b, 1c]. (Contact: Daiki Matsumaru, d-matsumaru@aist.go.jp).

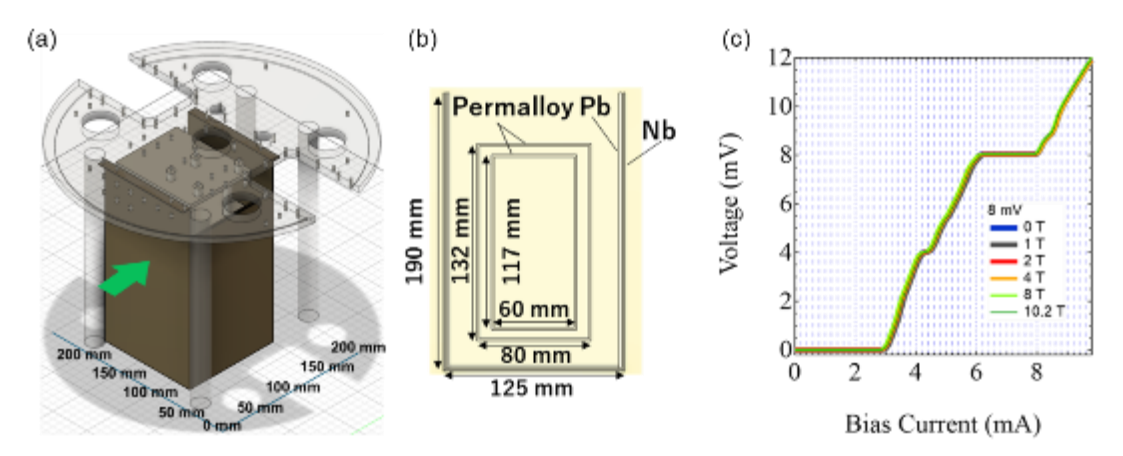


Fig.1-1 (a) Implementation of PJVS module with a superconducting shield structure in a dilution refriqerator. (b) Cross-sectional view of the magnetic shield structure. (c) Quantized voltage steps generated from the PJVS device coverd with the shielding structure placed in a magnetic-field environment near a strong magnet (~10 T) and a cancellation coil.

- D. Matsumaru, S. Nakamura, M. Maruyama, and N.-H. Kaneko, "Stable voltage generation with a Josephson voltage standard device cooled at a 4 K stage in a dilution refrigerator", *IEEE. Trans. Instrum. Meas.* Vol.72, No. 1004706, 2023.
- 1b. D. Matsumaru, T. Oe, S. Nakamura, M. Maruyama and N. -H. Kaneko, "Operation of Josephson voltage standard with superconducting shield in magnetic-field environment," 2024 Conference on Precision Electromagnetic Measurements (CPEM), Jul. 2024.
- 1c. D. Matsumaru, T. Oe, S. Nakamura, H. Yamamori, M. Maruyama and N.-H. Kaneko, "Assessing the effectiveness of superconducting magnetic shielding structures for the Josephson voltmeter," *The 37th International Symposium on Superconductivity (ISS2024)*, Dec. 2024.

2. Resistance

2.1 Standard Resistors

Development of compact and super extreme ultra-stable standard resistors from 1 Ω to 10 k Ω has been finished. We evaluated the characteristics of three 10 k Ω resistors, and







they showed quite stable behavior as shown below:

• Drift rate: around $\pm 15 \text{ n}\Omega/\Omega$ per year

• Temperature coeff.: $< 15 (n\Omega/\Omega)/K$

• Humidity coeff.: within $\pm 0.2 (n\Omega/\Omega)/\%$

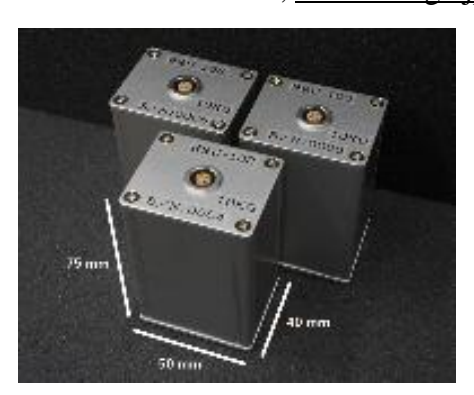
• Pressure coeff.: within $\pm 1 (n\Omega/\Omega)/100 \text{ hPa}$

The 10 k Ω resistors showed almost linear temperature characteristics from 18 °C to 28 °C and the temperature coefficients were less than 15 ($n\Omega/\Omega$)/K at 23 °C. The 10 k Ω resistors showed quite stable behavior within a few $n\Omega/\Omega$ even if exposed to temperature change of 5 °C. They showed about -5 $n\Omega/\Omega$ resistance change at the humidity of 72 %, but they were stable within a few $n\Omega/\Omega$ from 31 % to 52 %. The air pressure dependence was also evaluated under the pressure from 700 to 1200 hPa, and they also showed stable behavior within ± 10 $n\Omega/\Omega$. A vibration test along with a MIL standard, MIL-STD-202, was performed and the 2.5 k Ω sample showed stable behavior within 10 $n\Omega/\Omega$ after applying vibration for 2 hours on each axis (6 hours in total) [2a].

These excellent performances show that the developed resistors are suitable for utilization in national metrology institutes and international comparisons.

We are also working on the development of stable high-Ohm standard resistors with the Mitsubishi Gas Chemical Next Company, Inc. (formerly Japan Finechem Company) and they released new HVR10000 resistors. We evaluated the characteristics of the resistors from 10 T Ω to 1 P Ω , and the obtained drift rates were less than 8000 $\mu\Omega/\Omega$ for 1 P Ω resistors [2b]. Now, we are improving the resistors' overall performance.

(Contact: Takehiko Oe, t.oe@aist.go.jp).



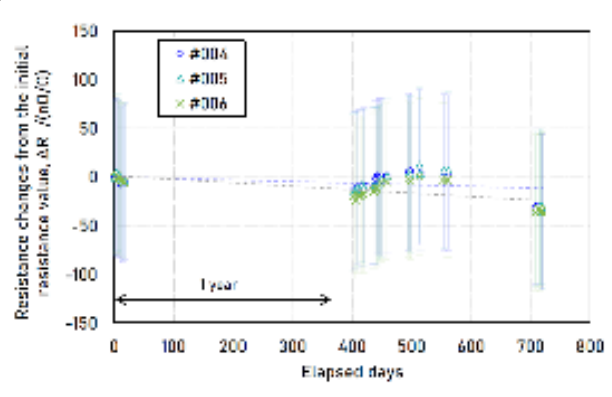


Fig. 2-1 Picture and the historical resistance data of developed 10 k Ω ultrastavle metal foil standard resistors. They shows stable behavior from just after the fabrication and the measured drift rate was less than ± 15 n Ω/Ω per year.









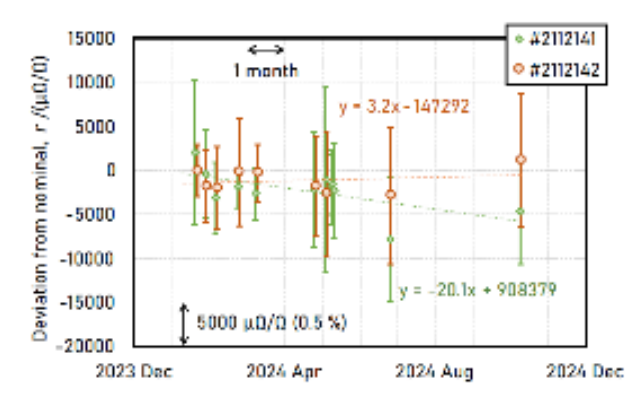


Fig. 2-2 Picture of the developed high-Ohm standard resistor, HVR10000 series made by Mitsubishi Gas Chemical Next Company Inc. The graph shows the historical resistance data of two 1 P Ω resistors.

2.2 DC high-resistance comparison between NIST and NMIJ

A precise high resistance comparison was performed between the traveling dual source bridge developed by the National Metrology Institute of Japan (NMIJ) and the adapted Wheatstone bridge of the National Institute of Standards and Technology (NIST) from 10 M Ω to 100 T Ω at NIST in 2019. The NMIJ traveling bridge was installed right next to the NIST bridge in Gaithersburg and these bridges alternately measured the resistance ratio of the high resistance standards, without moving the location of the resistors inside the temperature controlled-air-bath. Excellent agreement was obtained within the uncertainty of all resistance ranges and the difference between both systems was less than 1 $\mu\Omega/\Omega$ up to 1 T Ω and the degrees of equivalence for 10 T Ω and 100 T Ω were less than 6 $\mu\Omega/\Omega$ as shown in Fig. 2-3 [2a] (Contact: Takehiko Oe, t.oe@aist.go.jp).

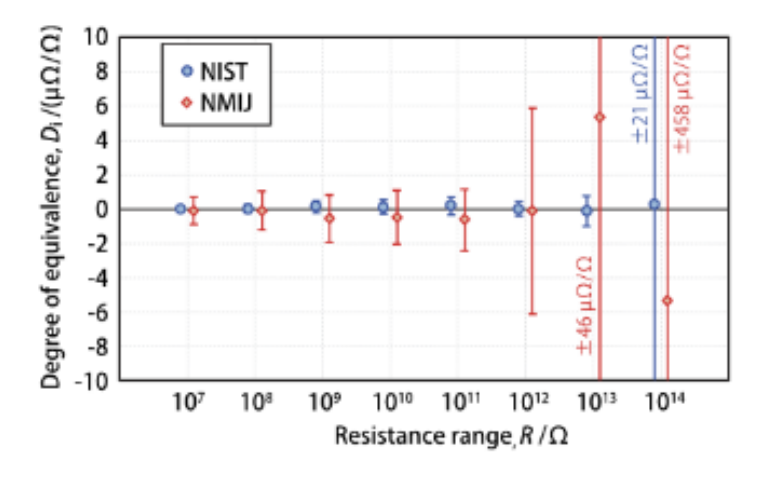


Fig. 2-3 .DoE for the measurements from 10 M Ω to 100 T Ω between NIST and NMIJ [2c].



2.3 Development of a next-generation quantum resistance standard

The unit of electrical resistance, Ω , is currently defined using the quantum Hall effect (QHE) as a primary standard. The QHE is a physical phenomenon in which the Hall resistance takes on a quantized resistance value when a strong magnetic field is applied perpendicular to a two-dimensional electron gas (formed on semiconductor interfaces or thin film materials). In the case of a two-dimensional electron gas utilizing a semiconductor hetero-interface such as GaAs, the required magnetic field is about 10 Tesla. To generate such a strong magnetic field, an electromagnet such as a superconducting solenoid is usually required, and the whole system including the refrigerator is large and expensive. Recently, a phenomenon called the quantum anomalous Hall effect (QAHE) has been discovered in a magnetic topological insulator. The QAHE originates from the exchange interaction between magnetic impurities inside the material and conduction electrons and does not require an external magnetic field. It is expected that a quantum resistance standard without strong magnetic field generators such as superconducting electromagnets will be realized by utilizing the QAHE.

We are currently conducting research toward realizing a quantum resistance standard that does not require a strong magnetic field generator by utilizing the QAHE. There are two challenges that must be solved when using the QAHE as a resistance standard. The QAHE is theoretically expected to take on a quantized resistance value when the Hall resistance value takes on a quantized resistance value, but it has yet been verified whether the quantized resistance value can be obtained in actual experiments. In addition, there is a problem of instability in which the quantization cannot be maintained by flowing a small amount of current for the measurement due to poor film quality of the magnetic topological insulator. To solve these problems, we have been working on high-precision Hall resistance measurement and improvement of film quality for the QAHE [2d]. Figure 2-4 shows a prototype of a quantum resistance standard based on a new principle that does not use a strong magnetic field generator, which was developed in collaboration with Riken [2e]. Precision Hall resistance measurements had revealed that ten parts-perbillion precision resistance standard, that is not inferior to the conventional QHE-based resistance standard, can be realized without using a strong magnetic field generator. (Contact: Yuma Okazaki, yuma.okazaki@aist.go.jp).





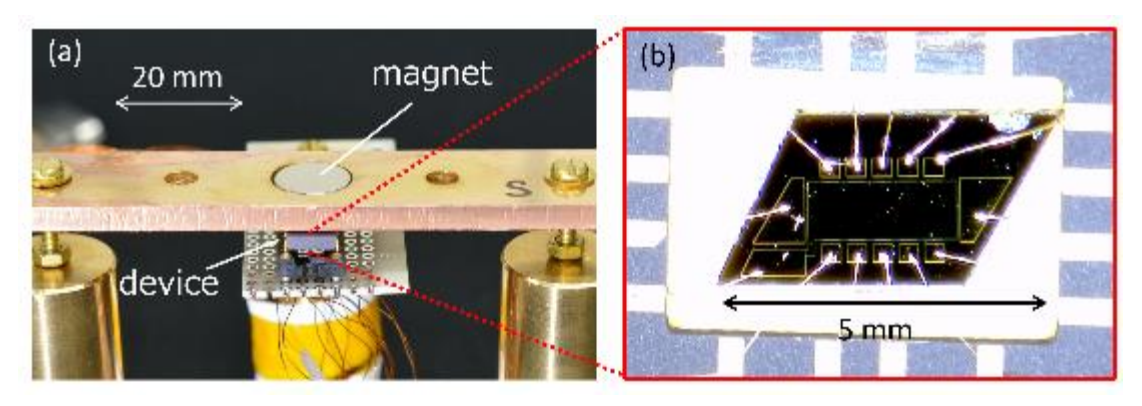


Fig. 2-4 (a) Photograph of a prototype of QAHE-based quantum resistance standard with a permanent disc magnet. (b) Microscope image of Hall bar device fabricated from a ferromagnetic topological insulator thin film.

- 2a. T. Oe, N.-H. Kaneko, M. Zama, and M. Kumagai, "Development of 10 k Ω metalfoil stable standard resistors", *CPEM2024 digest*.
- 2b. T.Oe, Y. Okazaki, T. Tanaka, N.-H. Kaneko, M. Yoshida, K. Tsuri, T. Kukisawa, "Development of stable high-resistance standard resistors", *CPEM2024 digest*.
- 2c. T. Oe, S. Payagala, A. R. Panna, S. Takada, N.-H. Kaneko, and D. G. Jarrett, "Precise high resistance comparison between the NMIJ traveling dual source bridge and the NIST adapted Wheatstone bridge", *Metrologia*, Vol. 59, No. 6, 065007, Oct. 2022.
- 2d. Y. Okazaki, T. Oe, M. Kawamura, R. Yoshimi, S. Nakamura, S. Takada, M. Mogi, K. S. Takahashi, A. Tsukazaki, M. Kawasaki, Y. Tokura, and N.-H. Kaneko, "Precise resistance measurement of quantum anomalous Hall effect in magnetic heterostructure film of topological insulator", *Appl. Phys. Lett.* 116, 143101, 2020
- 2e. Y. Okazaki, T. Oe, M. Kawamura, R. Yoshimi, S. Nakamura, S. Takada, M. Mogi, K. S. Takahashi, A. Tsukazaki, M. Kawasaki, Y. Tokura, and N.-H. Kaneko, "Quantum anomalous Hall effect with a permanent magnet defines a quantum resistance standard", *Nature Physics* 18, 25-29, 2022.

3. DC Current

3.1 Single Electron Pumping

Towards a realization of the current standard based on the single-electron pumping, we investigate the physics of low-temperature electron transport phenomena in various types of single-electron devices, i.e., superconductor-insulator-normal-insulator-superconductor (SINIS) turnstiles, gate-confined quantum dots, and graphene- or nanotube-based single-electron transistors.

On SINIS turnstiles, in our early studies, we had discovered the new phenomenon that is







a reduction of the single-electron pumping error induced by a weak magnetic field applied to the device [3a]. The origin of this phenomenon is related to the suppression of inverseproximity effect at the interface between superconducting leads and a normal metal island. The inverse proximity effect causes the quasiparticle trap at the interface, namely it leads to the overheating of the junction. The magnetic field weaken the inverse proximity effect and helps to lease the quasiparticle. We justify this scenario from numerical analysis and controlling the tunnel resistance. Aiming at further reducing the pumping error, we extended the research to that based on another pumping mechanism. In one instance, we investigated a GaAs-based gate-defined quantum dot and demonstrated single-parameter pumping. In addition, we developed an air-bridge based parallel integration of this pump to demonstrate a synchronized parallel pumping that can generate a larger current otherwise unattained. In this study, we succeeded to operate the GaAs single electron device with sigma-delta modulated pulses for the arbitrary wave generation [3b]. This technique is thought to be useful for the calibration of current noise in the shot noise measurement. Also, we start to measure the Si single electron pump device in collaboration with NTT group. At present we succeeded to operate single electron pumping at 1 GHz with 10^{-6} uncertainty. Also, we are trying to operate this type of device in parallel to generate large (a few nano ampere) current. Two silicon pump devices are simultaneously operated at 1 GHz with 10^{-6} uncertainty levels inside dilution refrigerator. To test the uncertainty of pumped current, we compared the generated current each other. As a result, we confirmed that the currents generated by the two devices agreed within an uncertainty of approximately 1 µA/A [3c].

These single-electron devices are planned to be integrated with the quantum metrology triangle experiment that combine the single-electron device with the quantum Hall resistance and Josephson voltage standards. Towards this futuristic experiment, we had introduced a dry dilution refrigerator; An ample open space offered by this refrigerator allows us to integrate the whole components required for the triangle experiment including a cryogenic current comparator into one system. Electric noise filters and high-frequency wiring are now designed and constructed to complete this setup. Also, to operate Josephson voltage standard and quantum Hall array device inside the dilution refrigerator, we are installing additional cold stage and try to operate these quantum standards. As a result, we succeeded to operate Josephson voltage standard inside a dilution refrigerator. We obtained 1 V with 2.4×10^{-10} and 2 mV with $2.1 \times \times 10^{-8}$ in the voltage measurement based on the Josephson voltage standard [1a]. (Contact: Shuji Nakamura, shuji.nakamura@aist.go.jp).





3.2 Development of ultrasmall current amplifier

We are currently developing a measurement instrument that can accurately measure femtoamperes (fA) and attoamperes (aA). Such ultra-small currents are important for measuring radiation dose rates using an ionization chamber, and it is required to accurately measure tiny currents of about 10 fA in radiation dose rate measurements of radiation sources used in cancer radiation therapy and environmental measurements of radiation and radioactivity. We developed a prototype using a stable ultra-high resistance element and evaluated the relative expanded uncertainty (corresponding to the 95 % confidence interval of the measured value) by measuring four different currents ranging from 0.7 fA to 330 fA [3d]. We performed similar measurements using two commercially available electrometers and compared their uncertainties as shown in Fig. 3-1. For all current values, our developed prototype can measure with excellent accuracy compared to commercially available electrometers 1 and 2. For instance, a current of 12 fA can be measured with a resolution of 46 aA. We will continue to develop this principle demonstration and realize more user-friendly micro-current measurements. (Contact: Yuma Okazaki, yuma.okazaki@aist.go.jp).

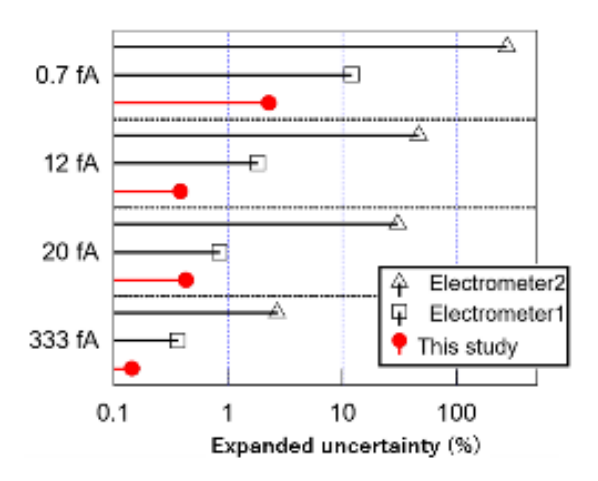


Fig. 3-1 Expanded uncertainty in ultrasmall current measurements. The results from our amplifier was compared with two commercially-available electrometers.

- 3a. S. Nakamura, Y. A. Pashkin, M. Taupin, V. F. Maisi, I. M. Khaymovich, A. S. Mel'nikov, J. T. Peltonen, J. P. Pekola, Y. Okazaki, S. Kashiwaya, S. Kawabata, A. S. Vasenko, J.-S. Tsai, and N.-H. Kaneko, "Interplay of the inverse proximity effect and magnetic field in out-of-equilibrium single-electron devices", *Phys. Rev. Appl.* 7, 054021, 2017.
- 3b. Y. Okazaki, S. Nakamura, K. Onomitsu, and N.-H. Kaneko, "Digital processing with single electrons for arbitrary waveform generation of current", *Appl. Phys. Express*







11, 036701, 2018

- 3c. S. Nakamura, D. Matsumaru, G. Yamahata, T. Oe, D.-H. Chae, Y. Okazaki, S. Takada, M. Maruyama, A. Fujiwara, and N.-H. Kaneko, *Nano Letters* 24 (1), 9-15
- 3d. Y. Okazaki, T. Tanaka, N. Saito, and N.-H. Kaneko, "Subfemtoampere resolved ionization current measurements using a high-resistance transimpedance amplifier", *IEEE Trans. Instrum. Meas.* Vol.71, 2002508, 2022

4. LF-Impedance

AC resistor calibration service has been kept in the range of $10 \text{ k}\Omega$ at 1 kHz. Standard capacitor (dry-nitrogen or fused silica dielectric) calibration service has been kept in the range of 10 pF up to 1000 pF at 1.592 kHz. (Contact: Norihiko Sakamoto, $\underline{\text{n-sakamoto@aist.go.jp}}$).

We are currently developing precision measuring techniques for diagnosis of the energy storage devices such as lithium-ion batteries and super-capacitors by using an impedance spectroscopy method. We have a plan to establish a metrology for evaluating the storage power devices. Preliminary impedance measurements for lithium-ion battery cells in the range of 10 mHz - 10 kHz demonstrated that the impedance value for unused cells is clearly distinguished from that for used-up cells. Impedance spectra for the unused cells which are obtained under 100 m Ω indicate that the evaluations of the uncertainties should be required for detecting a faint sign or a symptom of degradations of storage devices. We have developed an electrochemical impedance measurement system and have evaluated the type-A uncertainty for the impedance spectra which was estimated to be less than 0.2 m Ω .

AIST established the Global Zero Emission Research Center (GZR) in 2020. GZR has a mission for an international joint research base for zero emission technologies. GZR started to research for innovative environmental and energy technologies, including in the fields of renewable energy, storage batteries, hydrogen, and so on. NMIJ joined in GZR and has started the research of the safety and reliability evaluation method for solid oxide electrochemical cells and lithium-ion batteries by using precision impedance and charge-discharge measurements.

(Contact: Norihiko Sakamoto, <u>n-sakamoto@aist.go.jp</u>).







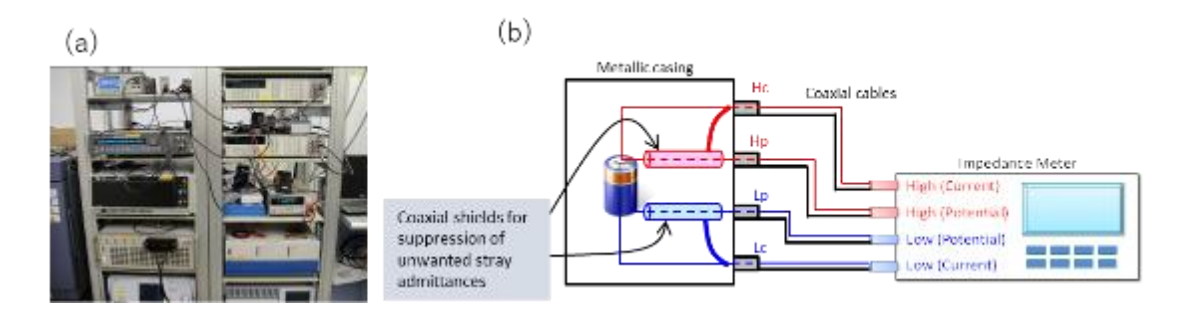


Fig. 4-1 (a)Photograph of the electrochemical impedance measurement system developed using the Frequency Response Analyzer and the Potentio-Galvano Stat. (b) Schematic of a impedance measurement network for a lithium-ion battery.

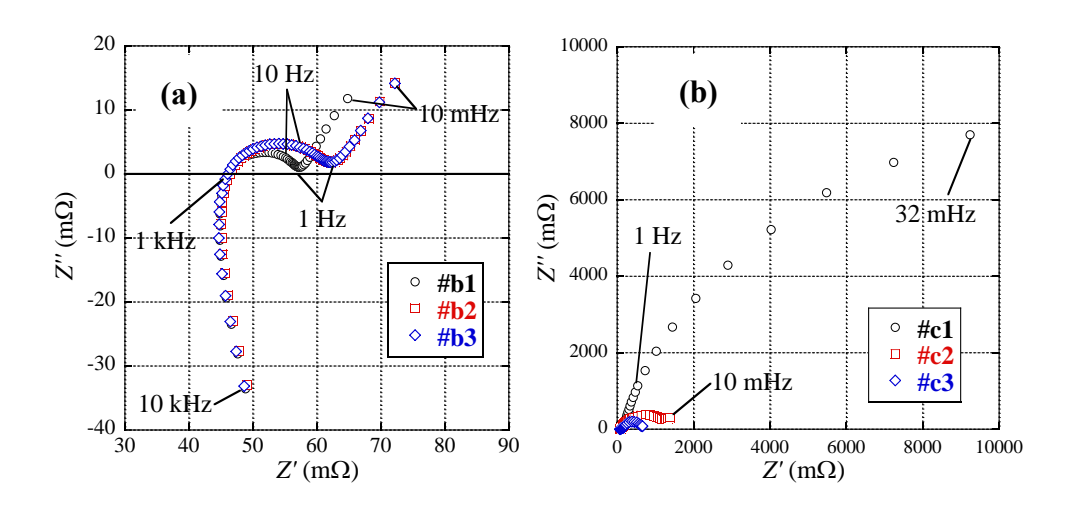


Fig. 4-2 Nyquist plot of the impedance spectra for the 18650-type lithium-ion batteries: (a) the unused samples and (b) used-up samples. Obvious change in impedance spectra was observed with the progression of the charge/discharge cycle.

5. AC/DC transfer

NMIJ has provided ac-dc voltage difference transfer calibration of thermal converters in the voltage range from 10 mV to 1000 V and in the frequency range from 10 Hz to 1 MHz, and AC voltage calibration below 10 Hz. We have been participating in APMP. EM-K12 comparison[5a], and CCEM-K6a/K9 key comparison[5b]. We will also participate in the new comparison, CCEM-K12.2025[5c].

The thin film multi-junction thermal converters with a novel design have been developed in collaboration with NIKKOHM co. ltd. We have introduced a new thermopile pattern



to improve the performance of our thin film MJTC[5d]. Using these thermal converters, novel thermal converter circuits arranged in a 2 by 2 matrix have been fabricated to improve the low-frequency AC-DC transfer differences[5e]. Thin-film AC-DC resistor on an aluminum nitride (AlN) substrate with negligible voltage dependence have been fabricated for measuring AC voltages up to 1000 V[5f]. Toward next-generation AC/DC current transfer standard, high-current multijunction thermal converters on a Si substrate up to 1 A have been designed and fabricated through the collaborative project with National Institute of Standards and Technology in Gaithersburg[5g].

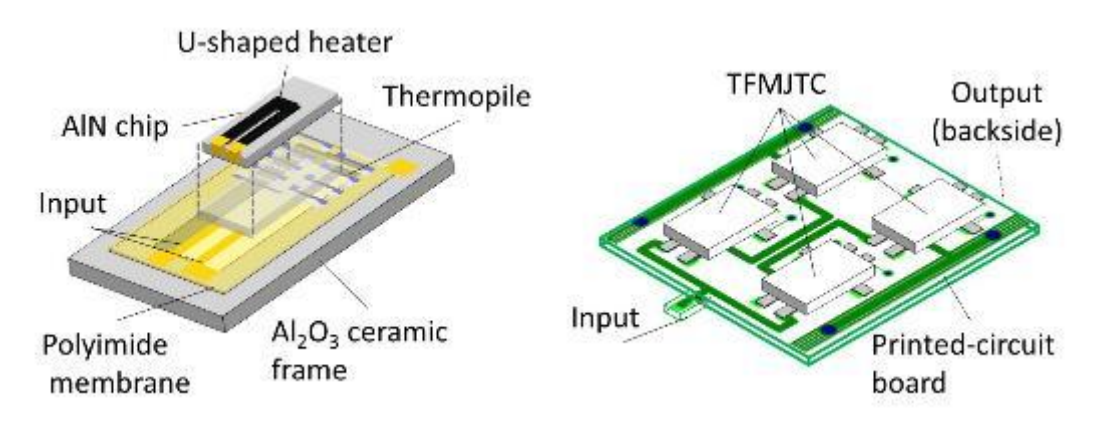


Fig. 5-1 A sheematic of the thermal current and voltage conveter developed at NMIJ.

Toward quantum AC voltage standards, a differential sampling measurement system using an AC-programmable Josephson voltage standard (AC-PJVS) system has been developed[5h]. To extend the voltage range of the system, we have combined a two-stage inductive voltage divider and a 10 V AC-programmable Josephson voltage standard chip.

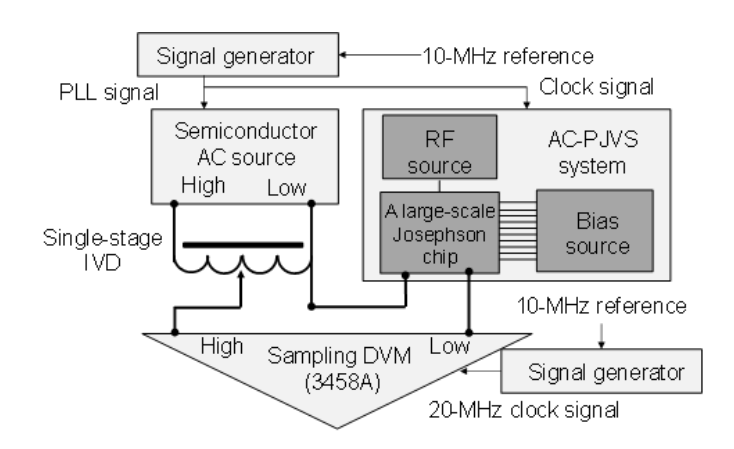


Fig. 5-2 Block diagram of calibration system with the AC-PJVS in the voltage range above 10 V.



Toward a waste-heat recovery with thermoelectric conversion, we have developed advanced metrology techniques and apparatus using a precise ac and dc electrical measurement technique. The Seebeck coefficient is an essential indicator of the conversion efficiency and the most widely measured property specific to these materials. So far, we have developed a method to precisely measure Thomson effect to determine the absolute Seebeck coefficient of platinum reference material[5i,5j]. We have also evaluated the direct measurement technique of the dimensionless thermoelectric figure of merit, zT, using ac and dc voltage measurements with a four-probe configuration[5k]. (Contact: Kenjiro Okawa, okawa.k@aist.go.jp, Yasutaka Amagai, y-amagai@aist.go.jp).

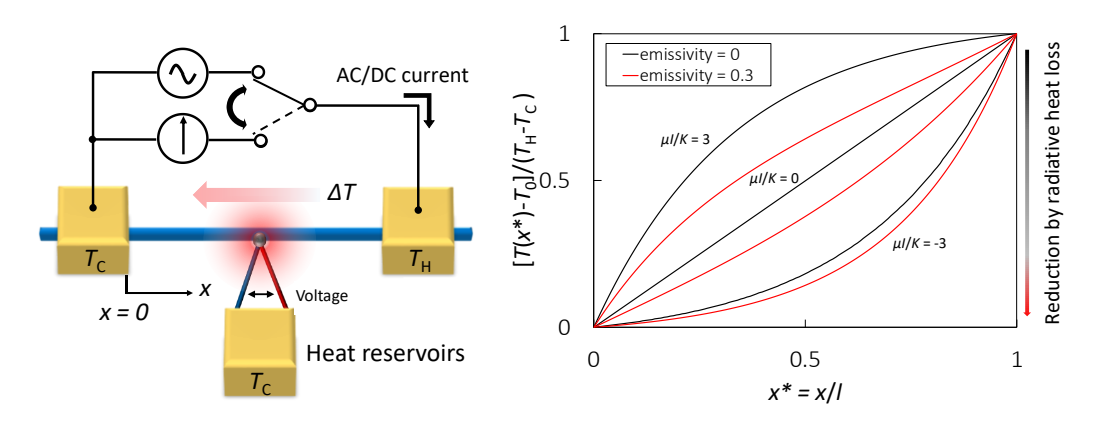


Fig. 5-3 A shcematic of the Thomson coefficient measuremnts of metallic wire.

- 5a. APMP. EM-K12, Key comparison of AC-DC current transfer standards. (https://www1.bipm.org/kcdb/comparison?id=509)
- 5b. CCEM-K6.a/K9, CIPM Key Comparison of AC-DC Voltage Transfer Standards.
- 5c. CCEM-K12, CIPM Key comparison of AC-DC current transfer standards.
- 5d. H. Fujiki, Y. Amagai, K. Shimizume, K. Kishino, S. Hidaka, "Fabrication of Thin Film Multijunction Thermal Converters With Improved Long-Term Stability," *IEEE. Trans. Instrum. Meas.* Vol.64, No.6, Jan. 2015.
- 5e. Y. Amagai, H. Fujiki, K. Okawa, N.-H. Kaneko, "Low-Frequency AC–DC Differences of a Series–Parallel Circuit of Thermal Converters," *IEEE. Trans. Instrum. Meas.* Vol.68, No.6. 2019.
- 5f. H.Fujiki, Y. Amagai, and K. Okawa, "Establishment of High-Voltage AC–DC Voltage Transfer Standards in 1–100-kHz Range at NMIJ," *IEEE. Trans. Instrum. Meas.* Vol.68, No.6. 2019.
- 5g. Y. Amagai, S. Cular. J. A. Hagmann, T. E. Lipe, N.-H. Kaneko "Low-Frequency Characteristics of Silicon-Based High-Current Multijunction Thermal Current Converters Fabricated by Wet Chemical Etching" *IEEE. Trans. Instrum. Meas.*







Vol.70, 2021.

- 5h. Y. Amagai, M. Maruyama, H. Yamamori, T. Shimazaki, K. Okawa, H. Fujiki, and N.-H. Kaneko, "Extending voltage range to 10 V rms in AC–DC difference measurements with AC programmable Josephson voltage standard" *Meas. Sci. Technol.* 31, 065010, 2020.
- 5i. Y. Amagai, T. Shimazaki, K. Okawa, T. Kawae, H. Fujiki, and N.-H. Kaneko, "High-accuracy compensation of radiative heat loss in Thomson coefficient measurement," *Appl. Phys. Lett.* Vol. 117, 063903, August 2020.
- 5j. Y. Amagai, T. Shimazaki, K. Okawa, T. Kawae, H. Fujiki, and N.-H. Kaneko, "Precise absolute Seebeck coefficient measurement and uncertainty analysis using high- *T*_c superconductors as a reference," *Rev. Sci. Instrum.* Vol.91, 14903, Jan. 2020.
- 5k. K. Okawa, Y. Amagai, N. Sakamoto, and N. -H. Kaneko, Measurement 232, 114626 (2024).

6. Power (NMIJ)

6.1. Power at NMIJ (harmonics, etc)

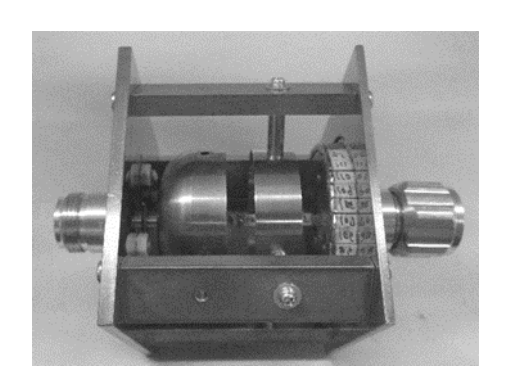
An improved evaluation system for a wideband resistive voltage divider (WRVD) is under development. The fabrication of an accurate and precise WRVD based on the extended Hamon method has been realized by direct soldering of series resistor and by soldering on the edge of round substrates for parallel resistor with suitable fixtures. The improved evaluation system was verified with calibrated IVDs. By replacing with a phase standard, the difference from the calibration result by Thompson's method has been effectively reduced comparing with the previous system. An error simulation of the equivalent circuit of the IVDs based on the calibration result has revealed the large quadrature error of the improved system at 50 kHz. It was considered due to the phase error of the phase standard.

We have launched a new project on developing a current comparator using a quantum magnetometer based on nitrogen-vacancy (NV) center in a diamond. The aim of this project is to pilot the future possibilities of the use of a NV-diamond magnetometer as a precise null detector of current comparator at the ultimate stage of quantum sensing-based current comparator development operatable at room temperature [6a]. (Contact: Tatsuji Yamada, yamada.79@aist.go.jp, Hidekazu Muramatsu, muramatsu.h@aist.go.jp)









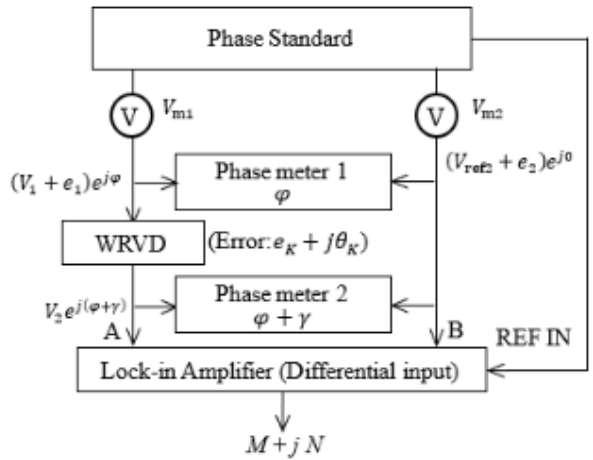


Fig. 6-1

6.2. Power at JEMIC (mains)

JEMIC has provided the primary active/reactive power/energy standards for the power frequencies in the voltage range from 50 V to 120 V and in the current range from 2.5 A to 50 A. The standard individually measures voltage U and current I with two precise voltmeters and a shunt resistor, and phase θ with a precise digital phase meter. After these measurements, the active and reactive powers are calculated from $UI\cos\theta$ and $UI\sin\theta$, respectively. The representative expanded uncertainties under conditions of 100 V and 5 A are 22 μ W/VA (power factor 1) and 10 μ W/VA (power factor 0). In 2023, we calibrated about 10 power meters and 20 energy meters. JEMIC has been participating in APMP Key Comparison for APMP.EM-K5.1 of AC power and energy[6b]. (Contact: TADOKORO Takuya, t-tadokoro@jemic.go.jp)

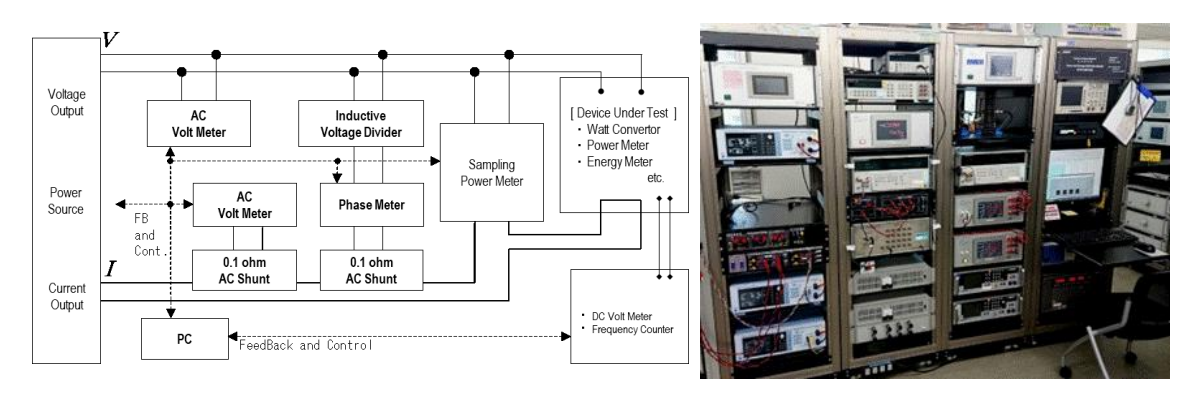


Fig. 6-2

6a. H. Muramatsu *et al.*, "Diamond Quantum Magnetic Sensor toward a Precision Comparison of Currents with a Current Comparator," 2024 Conference on Precision





Electromagnetic Measurements (CPEM), Denver, CO, USA, 2024, pp. 1-2.

6b. https://www.bipm.org/kcdb/comparison?id=198

7. RF-Power

The previously developed waveguide calorimeter in the WR-5 band was improved (Fig. 7-1) [7a]. The improved calorimeter employs a newly designed adiabatic waveguide which has the same level of thermal insulation, lower transmission loss and smaller heat capacity than the conventional one. NMIJ has created a 3D-printed absorber for efficient and fast detection of terahertz waves in the frequency range expected to be used in 6G mobile communication system [7b]. A resin absorber with hollow pyramid structures was fabricated using a 3D printer. This hollow-type absorber contributes to improved calorimetric time constants due to its low heat capacity. Then we form a thin metal film on the surface of the resin, thinner than the skin depth of the electromagnetic waves, to act as an absorbing layer. These results are expected to improve the performance of absorbers for free-space and waveguide calorimeters in the future.



Fig.7-1 Photograph of the developed adiabatic waveguide. Conventional type (left) and new type (right).

(Contact: Yuya Tojima, yuya-tojima@aist.go.jp, Moto Kinoshita, moto-kinoshita @aist.go.jp)

- 7a. Y. Tojima, M. Kinoshita and M. J. Yamamoto, "Improvement of the WR-5 Calorimeter at NMIJ Using a Novel Adiabatic Waveguide," 2024 Conference on Precision Electromagnetic Measurements (CPEM), Denver, CO, USA, 2024, pp. 1-2, doi: 10.1109/CPEM61406.2024.10645989.
- 7b. Kuwano, G., Kurihara, K., Hokari, R. et al. 3D Printed Broadband Sub-terahertz Absorber for Absolute Power Sensors in Free Space. J Infrared Milli Terahz Waves 45, 592–603 (2024). https://doi.org/10.1007/s10762-024-00996-9.





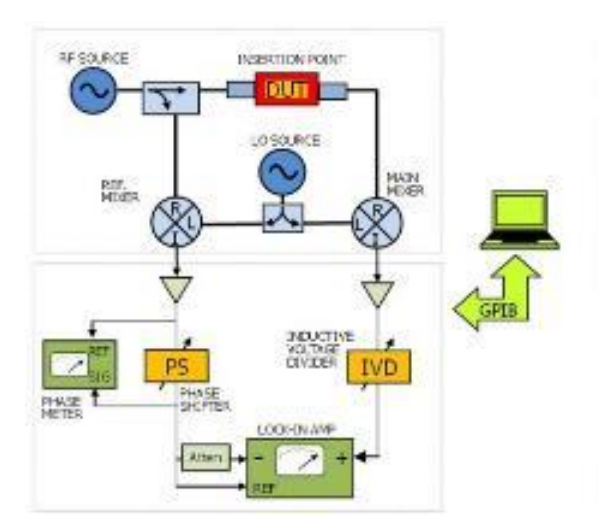


8. RF-Attenuation and Phase Shift

NMIJ has established national standard for RF and microwave attenuation in the frequency range of 1 kHz to 110 GHz and provides its calibration services mainly with the Japan Calibration Service System (JCSS) scheme. All measurement and calibration systems work based the intermediate frequency (IF) substitution method using the highly accurate null detection and employing an inductive voltage divider (IVD) as the reference standard. A recent improvement was the inclusion of a new measurement system in the frequency range of 1 kHz to 100 kHz, to meet requirements industry for electromagnetic compatibility (EMC) [8a]. These systems have been commercially manufactured by 7Gaa Corporation (https://7gaa.co.jp/) and several have been shipped to overseas NMIs for use as their national RF attenuation standards (Fig.8-1). A very simple but accurate technique has been developed for RF and microwaves high-



Fig. 8-1 Photograph of the commercialized NMIJ RF/MW attenuation measurement system.



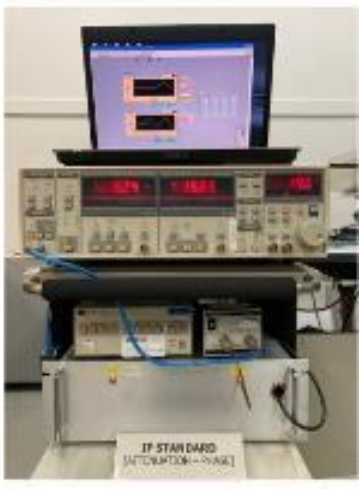


Fig. 8-2 Block diagram of the primary standard system for RF/MW attenuation and phase-shift (left) and picture of its working standard system. (right).





attenuation by using a new double-step technique without the use of external gauge block attenuator [8b].

NMIJ also established national standard for RF and microwave phase shift in the frequency range of 10 MHz to 50 GHz to meet industry demands in the field of 5G/6G wireless technologies as well as advanced radar technologies used such as in emergency braking systems, etc., where accurate phase shift measurements are as important as amplitude or attenuation measurements. This standard consists of two systems; the primary standard which uses a highly accurate null detection technique and the working standard which uses a multi-purpose lock in amplifier as a detector (Fig.8-2) [8c, 8d].

NMIJ took an initiative to organize a CIPM Key Comparison of attenuation at 18 GHz, 26.5 GHz and 40 GHz using a step attenuator (CCEM.RF-K26). Fourteen National Metrology Institutions (NMIs) participated in this key comparison, and successfully determined the Key Comparison Reference Values (KCRVs). The results reported by each NMI were then related to the KCRVs by calculating the Degree of Equivalence (DoE) and their expanded uncertainties (Fig.8-3) [8e, 8f]. NMIJ contributed significantly to this comparison by providing excellent measurement results.

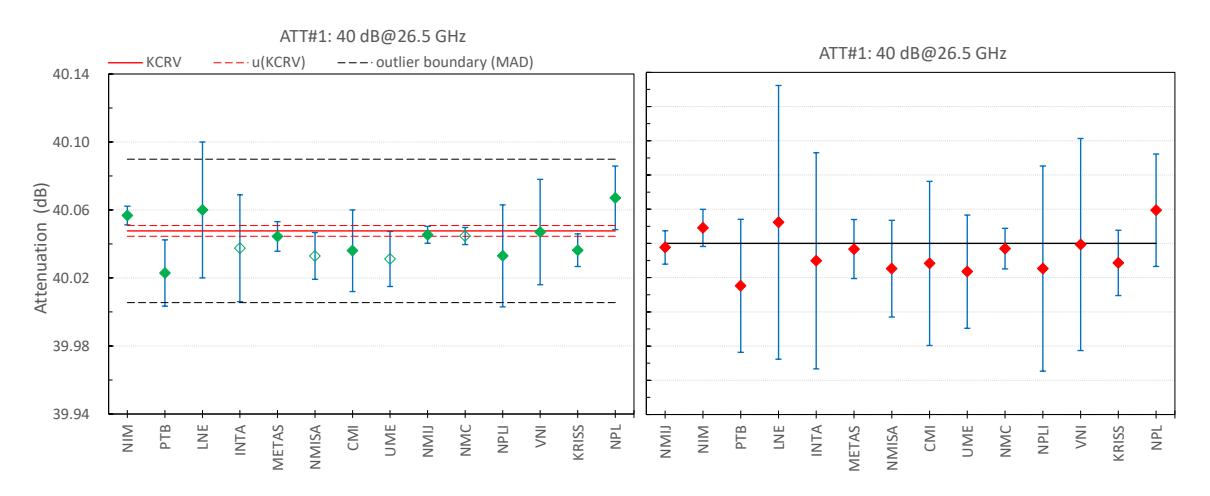
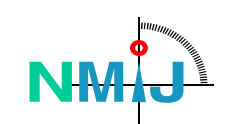


Fig. 8-3 Result of 40 dB incremental attenuation of the Transfer Standard ATT#2 at 26.5 GHz. Measurements results and the Key Comparison Reverence Value (KCRV) obtained (left). Degree of Equivalence (DoE) (right).

(Contact: Anton Widarta, anton-widarta@aist.go.jp, Moto Kinoshita, moto-kinoshita@aist.go.jp)

8a. A. Widarta, "Primary standard of attenuation in the frequency range of 1 kHz to 10 MHz," in CPEM Dig., Denver, Co, Aug. 2020, virtual.







- 8b. A. Widarta, "Double Step Technique for Accurate Microwave High Attenuation Measurements," IEICE Trans. Electron, vol.LE107–C, no.10, pp. 349-354, Oct. 2024
- 8c. A. Widarta, "Null technique for precision RF phase shift measurements," IEEE Trans. Instrum. Meas., vol. 68, no. 6, pp. 1840–1843, Jun. 2019.
- 8d. A. Widarta, "Working Standard for RF Attenuation and Phase-shift Calibrations," in CPEM Dig., Wellington, NZ, Dec. 2022.
- 8e. A. Widarta, "CCEM key comparison CCEM.RF-K26. Attenuation at 18 GHz, 26.5 GHz and 40 GHz using a step attenuator. Final report of the pilot laboratory," Metrologia, vol. 61, no. 1A, Jan. 2024.
- 8f. https://www.bipm.org/documents/d/guest/ccem-rf-k26

9. RF-Impedance and related measurement technology

NMIJ researched the precision on-wafer measurement techniques over 300 GHz and developed a full-automatic RF probing system establishing high reproducibility of measurements. Furthermore, electromagnetic sensing techniques is also researching for the agriculture products, food and infrastructure, etc.

NMIJ as a pilot laboratory has submitted the final report of the CCEM key comparison (CCEM.RF-K5c.CL: S-parameter for PC3.5 in the range from 50 MHz to 33 GHz) [9a], is creating the draft report of the APMP supplemental comparison (APMP.EM.RF-S5.CL: Dimensionally-derived characteristic impedance for PC7, PC2.4 and PC1.85) [9b].

Calibration certificates for S-parameter using the vector network analyzers and using dimensional measurement systems have been digitized.

(Contact: Ryoko Kishikawa, ryoko-kishikawa@aist.go.jp, Seitaro Kon, <u>seitaro-kon@aist.go.jp</u>)

- 9a. https://www.bipm.org/kcdb/comparison?id=599
- 9b. https://www.bipm.org/kcdb/comparison?id=333

10. Antennas

A calibration service for the free-space antenna factor on loop antenna is maintained in the frequency range of 20 Hz to 30 MHz. The expanded uncertainty of the magnetic antenna factor is from 0.4 dB to 0.7 dB in the frequency range from 9 kHz to 30 MHz [10a, 10b]





Calibration of the dipole antenna factor above a ground plane from 30 MHz to 1 GHz with the specific conditions (with horizontal polarization and at 2.0 m from the ground plane surface) is available. The open-area test site at NMIJ/AIST has been refreshed by reconstructing its ground plane. The flatness of the ground plane has been improved so that the 1 m grid measurement points over the ground plane are all fall in ± 6 mm. The site quality is under investigation. Since EMC (electromagnetic compatibility) measurements are ordinarily carried out in free space above 1 GHz, the dipole antenna factor from 1 GHz to 2 GHz is calibrated in an anechoic chamber. The free space dipole factor is one of the traceability source of the E-field strength calibration in free space.

(Contact: Takehiro Morioka, <u>t-morioka@aist.go.jp</u>, <u>Nao Takahashi, nao-takahashi@aist.go.jp</u>)



Fig. 10-1 Refreshed open-area test site at NMIJ/AIST.

The free space antenna factor calibration services for broadband antenna for Biconical antenna (30 MHz to 300 MHz), Log periodic dipole array antenna (300 MHz to 1000 MHz) and Super broadband antenna (30 MHz to 1000 MHz) are being performed using our original three antenna calibration method [10c-10d]. The ten calibration services have been provided to the client in between 2019 and 2021. In 2022, we digitized calibration certificates for broadband antennas and provided the client with four digitized calibration certificates.

(Contact: Sayaka Matsukawa, sayaka-matsukawa@aist.go.jp)







Calibration services for the gains of standard horn antennas are being performed from 18 GHz to 40 GHz using the extrapolation method. An antenna factor calibration service for the broadband horn antenna (1 GHz to 18 GHz) is available using the time-domain single antenna extrapolation method in the semi-anechoic chamber [10e].

(Contact: Yuanfeng She, yuanfeng.she@aist.go.jp)

An antenna gain calibration service for millimeter-wave standard gain horn antenna are being performed form 50 GHz to 75 GHz and 75 GHz to 110 GHz using a time-domain processing and extrapolation technique. Standard gain horn antenna calibration service for 220 GHz to 330 GHz has been started from March 2020. The expanded uncertainty of antenna gain was estimated to between 0.34 dB to 0.5 dB. The mm-wave antenna gain calibration by single antenna extrapolation method with moving flat-reflector is also studied [10f-10g].

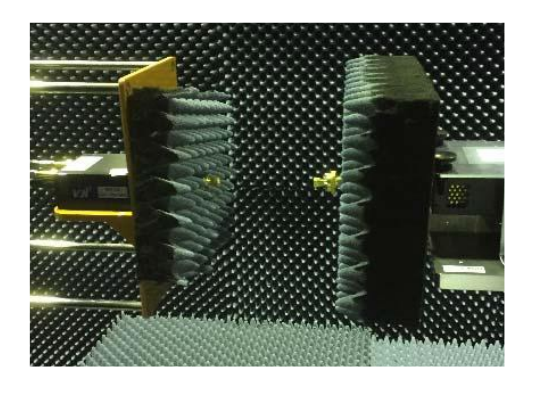


Fig. 10-2 Antenna gain calibration system compare for 220 to 330 GHz.

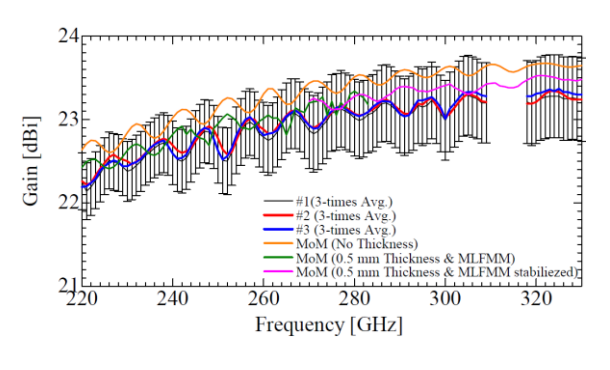


Fig. 10-3 Estimated antenna gain that with MoM results.

10a.https://www.bipm.org/kcdb/comparison?id=245

10b.M. Ishii, "Improvement of Uncertainty in Calibrating Primary Standard Loop Antenna by Three-antenna Method," 2022 Conference on Precision Electromagnetic Measurements (CPEM), Dec. 2022.

10c.S. Matsukawa and S. Kurokawa, "Antenna gain self-calibration for Double Ridged Guide Horn Antenna using bi-directional optical fiber link transceiver", ECTI-CON2019, pp. 1-4, Pattaya, Thailand, 10-13 July 2019.

10d.S. Matsukawa, S. Kurokawa and, M. Hirose, "Uncertainty Analysis of Far-Field Gain Measurement of DRGH Using the Single-Antenna Method and Amplitude Center Distance", IEEE Tran. on Instrumentation and Measurement, Vol. 68, No. 6, pp. 1756-1754, June 2019.



- 10e.Y. She, S. Matsukawa, S. Kurokawa, "Uncertainty Analysis of Far-Field Gain Measurement of DRGH Using Single-Antenna Extrapolation Method from 1 GHz to 18 GHz," 2022 MJWRT, Malaysia, Jan, 2022 (Hybrid workshop).
- 10f. M. Ameya and S. Kurokawa, "Development of Antenna Gain Calibration System in 300 GHz Frequency Band", Proceedings of 2019 URSI-Japan Radio Science Meeting, A2-4, 2019.
- 10g.M. Ameya, S. Matsukawa, and S. Kurokawa, "Uncertainty Estimation of Antenna Gain Self-Calibration Method with Moving Flat Reflector for 5G Standard Gain Horn Antenna", Proceedings of IEEE CAMA 2019, pp.277-280, 2019.

11. Electromagnetic fields

The E-field strength is one of the important quantities in the electromagnetic free field metrology, and the field measurement is ordinarily carried out by using a calibrated E-field probe. In NMIJ/AIST, the correction factors of the E-field probe are calibrated against the field level of 10 V/m and 20 V/m generated in a G-TEM cell. Three appropriate methods to generate the standard E-field are employed in calibrating the response of the primary optical field transfer probe depending on the measurement frequency. A TEM cell is employed as a standard E-field generator at lower frequencies below 900 MHz, and the E-field level in the frequency range from 0.8 GHz to 2.2 GHz is calibrated by using the free space dipole antenna factor in the anechoic chamber. Antenna gain and the net power flowing into the transmitting antenna are the traceability sources for the standard field generation in the anechoic chamber from 2 GHz to 6 GHz. The optical E-field transfer probe calibrated against these standard E-fields is used for the E-field level calibration in the G-TEM cell [11a, b].

(Contact: Takehiro Morioka, t-morioka@aist.go.jp)

AC Magnetic field sensor calibration service is maintained in a range of 1 uT to 150 uT from 50 Hz to 100 kHz. The realizable field strength depends on frequency points.

NMIJ is also developing a novel EM-sensor and a EM visualization method by using quantum phenomena of vapor cesium atoms [11c].

(Contact: Masanori Ishii, masanori-ishii@aist.go.jp)

- 11a.T. Morioka, "Systematic and random errors in the net power measurement using a reflectometer," IEEE Trans. Instrum. Meas., vol. 70, 1010110, Sep. 2021.
- 11b.T. Morioka, "Calibration of an Optical E-Field Transfer Probe," in Proc. Of 2024 IEEE Joint Int. Symp. On EMC, SPI: EMC Japan/APEMC, p.84, Okinawa, Japan,







May 2024.

11c.M. Ishii, "A Feasibility Study of AC Magnetic Field Sensor in kHz-band Based on Quantum Phenomena in 133Cs," 2022 Conference on Precision Electromagnetic Measurements (CPEM), Dec. 2022.

12. Electromagnetic radiation and scattering properties

Radar Cross Section (RCS) calibration service for cylindrical metal reflector and square metal plate in W-band has been started from March 2019 (Fig. 12-1). The expanded uncertainty of RCS for cylindrical metal reflector in W-band was estimated to between 1.1 to 1.6 dB. The expanded uncertainty of RCS for square metal plate reflector in W-band was estimated to between 1.4 dB to 2.1 dB.

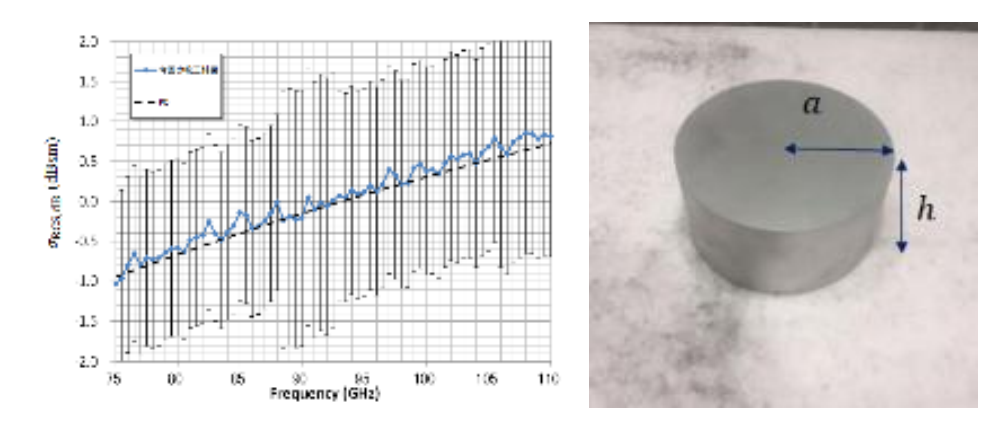


Fig. 12-1 RCS calibration results in W-band and an example of a cylindrical reflector.

(Contact: Michitaka Ameya, m.ameya@aist.go.jp)

The CATR (Compact Antenna Test Range) facility has been developed for 5G/6G antenna radiation pattern measurement and RCS pattern measurement for 5G/6G metasurface in the frequency range from 100 GHz to 330 GHz (Fig. 12-2). The RCS measurement results of a metasurface have been published in reference [12a].

(Contact: Michitaka Ameya, m.ameya@aist.go.jp, Yuto Kato, y-katou@aist.go.jp)

12a. Yuto Kato, Michitaka Ameya, et.al., "220/293 GHz Dual-Band Anomalous Reflectors Using Higher-Order Diffraction Modes and Their Precise Characterization Using a Compact Antenna Test Range System", IEEE Access, vol. 11, pp. 139295-139305, 2023







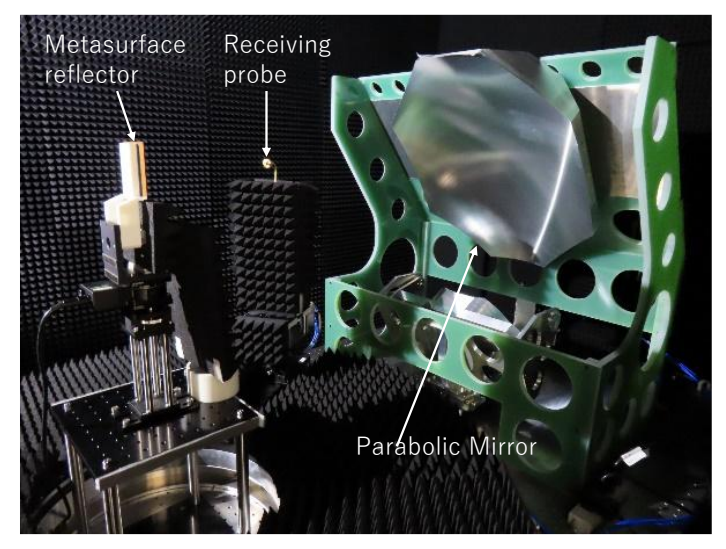


Fig. 12-2 CATR system for 5G/6G antenna radiation pattern measurement and RCS pattern measurement.

13. Material Characterization

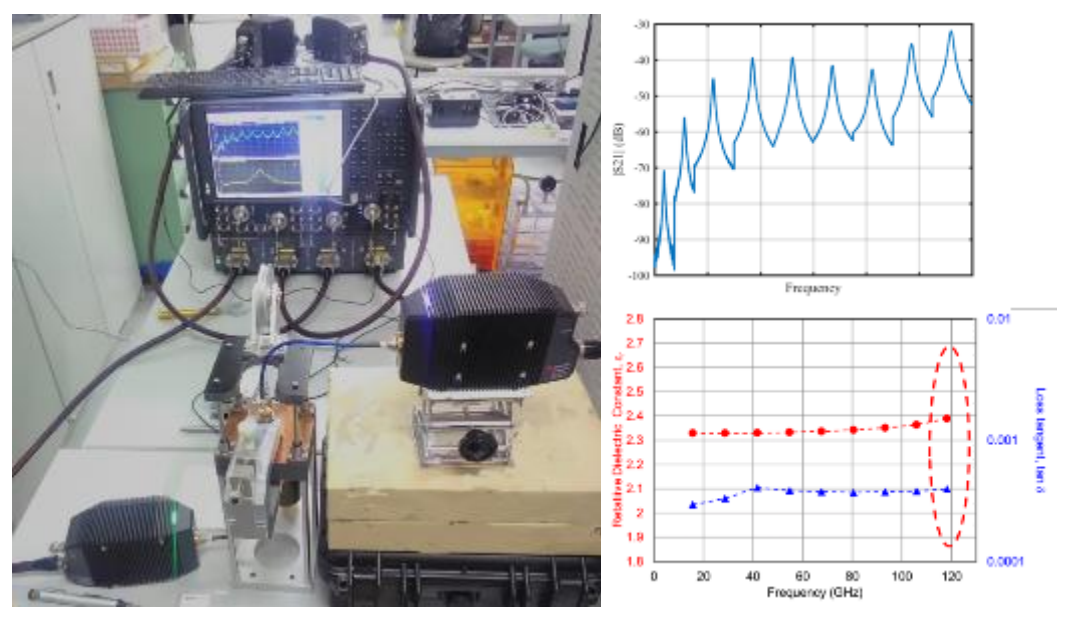


Fig. 13-1 Photographs of Balanced-type circular-disk resonator(BCDR) and Measurement Results of cyclic olefin polymers (COP) up to 120 GHz.

NMIJ has developed material characterization technique in the millimeter-wave and subterahertz frequency bands by using the balanced-type circular disk resonator (BCDR) [13a, 13b]. The technique can provide complex permittivity and conductivity measurements of low-loss dielectric substrate materials. The BCDR-based complex permittivity measurement method has already been standardized in IEC (IEC 63185: 2020), and the standardization for the conductivity measurements is under consideration.



The BCDR system supporting complex permittivity and conductivity measurements up to 120 GHz has been commercialized by a measurement instrument company (Fig. 13-1) [13c]. Moreover, NMIJ has successfully demonstrated increasing the measurement frequency of the BCDR-based material characterization in the D-band with a modified full-wave modal analysis [13d].

Furthermore, NMIJ has managed a pilot study on material characterization in the microwave and millimeter-wave bands as a pilot laboratory [13e].

(Contact: Yuto Kato, y-katou@aist.go.jp, Seitaro Kon, seitaro-kon@aist.go.jp))

- 13a. Y. Kato, M. Horibe, "Broadband complex permittivity and conductivity measurements in the millimeter-wave bands over variable temperatures using a balanced-type circular disk resonator," Appl. Phys. Lett. 30 August 2021; 119 (9): 092902.https://doi.org/10.1063/5.0055471
- 13b.Y. Kato and M. Horibe, "Broadband Conductivity Measurement Technique at Millimeter-Wave Bands Using a Balanced-Type Circular Disk Resonator," IEEE Transactions on Microwave Theory and Techniques, vol. 69, no. 1, pp. 861-873, Jan. 2021.
- 13c. Keysight Technologies, "N1501AE11/67 Balanced Type Circular Disk Resonator (BCDR)," https://www.keysight.com/us/en/assets/7120-1214/ flyers/N1501AE11-67-Balanced-Type-Circular-Disk-Resonator-BCDR. pdf.
- 13d. Y. Kato, "D-Band Material Characterization Using a Balanced-Type Circular Disk Resonator With Waveguide Interfaces and a Modified Full-Wave Modal Analysis," IEEE Transactions on Instrumentation and Measurement, vol. 72, pp. 1-10, 2023, Art no. 6009210.
- 13e. "CCEM Pilot Study on dielectric material measurement," https://www.bipm.org/documents/20126/125885563/CCEM.RF-P1.

14. RF-Quantum Measurements

NMIJ conducts research into the quantum measurement of electromagnetic waves. Recently, a method has been developed to measure microwave attenuation using the Rabi frequency of cesium atoms, called "Rabi attenuation". The linearity of the microwave intensity based on the Rabi frequency was significantly improved by accurately evaluating the detuning of the resonance frequency of cesium atoms, and we also found that the spatial inhomogeneity of the microwaves is a major cause of the residual non-linearity. These results were presented at CPEM2024 [14a]. We also reported on the power measurements, attenuation measurements, antenna measurements, frequency

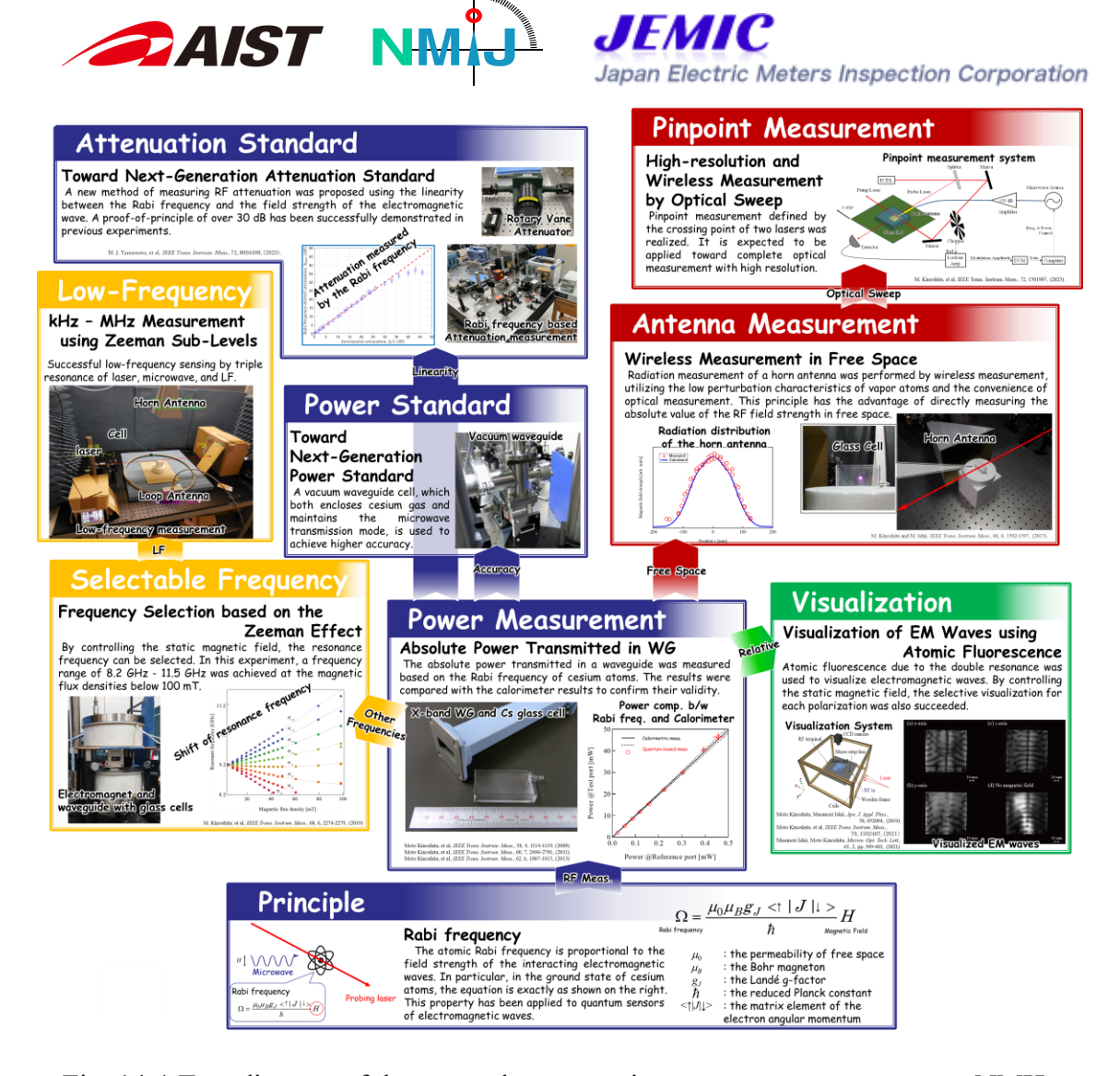


Fig. 14-1 Tree diagram of the research progress in quantum measurements at NMIJ.

arbitrariness and visualization of electromagnetic waves that NMIJ has carried out so far in relation to quantum measurements of microwaves [14b]. Figure 14-1 shows a tree diagram of the research progress in quantum measurements at NMIJ. The quantum measurements of electromagnetic waves at NMIJ has been developed into the attenuation measurement and the antenna measurement, with the main focus on the precision of the power of cesium atoms with Rabi frequencies. It has also been applied to the development of frequency tunability using various quantum states and the visualization of electromagnetic waves using fluorescence.

(Contact: Moto Kinoshita, moto-kinoshita@aist.go.jp)

14a. M. J. Yamamoto, Y. Tojima and M. Kinoshita, "Improving Rabi Attenuation: Toward a Quantum-Based Microwave Attenuation Standard with Atomic Vapor," 2024







Conference on Precision Electromagnetic Measurements (CPEM), Denver, CO, USA, 2024, pp. 1-2, doi: 10.1109/CPEM61406.2024.10646094.

14b.M. Kinoshita, Y. Tojima, M. J. Yamamoto and M. Ishii, "Research progress of electromagnetic wave measurement using cesium atoms at NMIJ," *2024 Conference on Precision Electromagnetic Measurements (CPEM)*, Denver, CO, USA, 2024, pp. 1-2, doi: 10.1109/CPEM61406.2024.10646006.

15. Digitalization

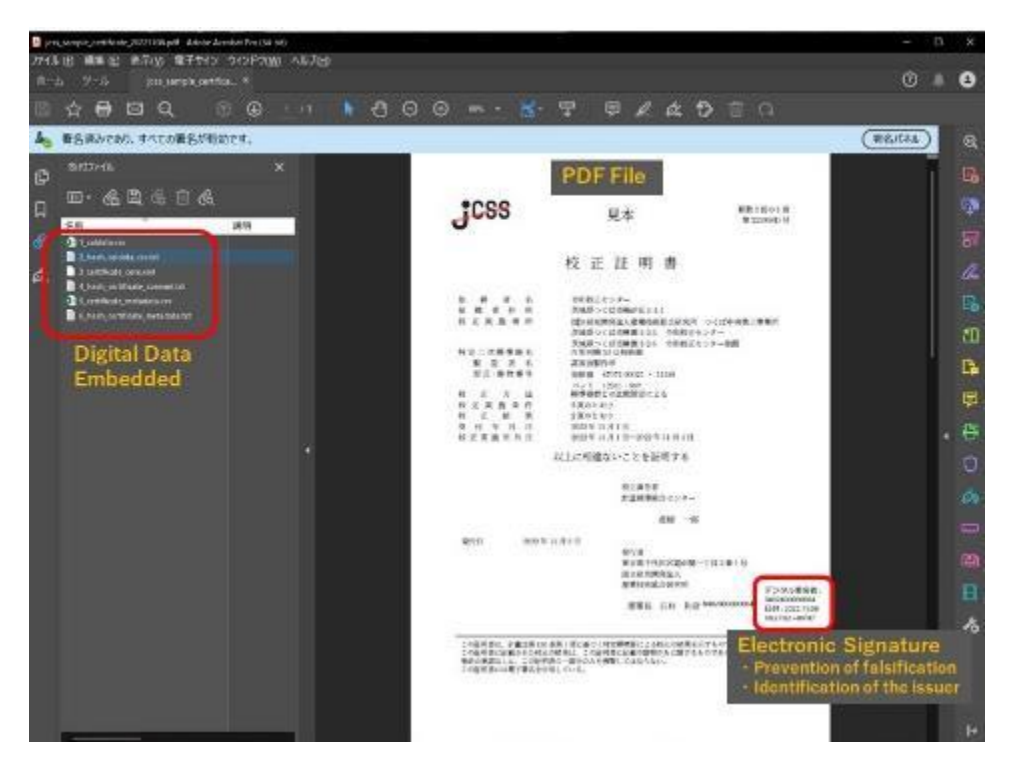


Fig. 12-1 A sample of NMIJ's DCC. The DCC is based on PDF with digital data embedded and secured by an electronic signagture.

NMIJ has started issuing Digital Calibration Certificates (DCCs) with the PDF format. NMIJ's DCCs look similar to the conventional calibration certificates issued in the paper format, but for customer convenience, digital data such as calibration metadata and calibration results are also embedded in CSV format (Fig. 12-1) to the PDF files of DCCs. NMIJ allows customers to choose between paper calibration certificates and DCCs when applying for calibration, and many customers in the field of electrical standards choose DCCs.